



# Old carbon, new insights: thermal reactivity and bioavailability of saltmarsh soils

Alex Houston<sup>1</sup>, Mark H. Garnett<sup>2</sup>, and William E. N. Austin<sup>1,3</sup>

<sup>1</sup>Department of Geography and Sustainable Development, University of St Andrews,  
St Andrews, KY16 9AL, United Kingdom

<sup>2</sup>NEIF Radiocarbon Laboratory, Scottish Universities Environmental Research Centre,  
East Kilbride, G75 0QF, United Kingdom

<sup>3</sup>Scottish Association of Marine Science, Oban, PA37 1QA, United Kingdom

**Correspondence:** Alex Houston (ah383@st-andrews.ac.uk)

Received: 21 October 2024 – Discussion started: 13 November 2024

Revised: 14 July 2025 – Accepted: 4 August 2025 – Published: 23 September 2025

**Abstract.** Saltmarshes are globally important coastal wetlands which can help to mitigate the impacts of climate change. They accumulate organic carbon from both modern and aged sources through in-situ biological production and the capture of ex-situ sources which are deposited during tidal inundation. Previous studies have found that long-term organic carbon storage in saltmarsh soils is driven by the net contribution from the older fraction, implying that the inputs of young organic carbon derived from in situ production are recycled at a faster rate.

Using ramped oxidation, we assessed the composition ( $^{14}\text{C}$  and  $^{13}\text{C}$ ) of saltmarsh soil carbon pools defined by their thermal reactivity. By relating  $^{14}\text{C}$  measurements of the soil carbon pools to  $\text{CO}_2$  respired in aerobic incubations of the same soils, we provide the first empirical evidence linking the thermal reactivity of saltmarsh soil organic carbon with its bioavailability for remineralization.

We found that old ( $^{14}\text{C}$ -depleted) carbon dominates the thermally recalcitrant organic carbon pools, whereas the thermally labile carbon is composed of younger organic carbon sources. In most cases, the  $^{14}\text{C}$  content of the most thermally labile carbon pool was closest to the previously reported  $^{14}\text{C}$  content of the  $\text{CO}_2$  evolved from aerobic incubations of the same soils, implying that the bioavailability of saltmarsh soil organic carbon to remineralisation in oxic conditions is closely related to its thermal lability.

Our results highlight the importance of saltmarshes as stores of both old, thermally recalcitrant organic carbon, as well as younger, thermally labile organic carbon that is vul-

nerable to decomposition under oxic conditions. Management interventions (e.g. rewetting by tidal inundation) to limit the exposure of saltmarsh soils to elevated oxygen availability may help to protect and conserve these stores of thermally labile organic carbon and hence limit  $\text{CO}_2$  emissions. We also present evidence to support the inclusion of thermally labile allochthonous OC stored in saltmarsh soils in additionality assessments for projects which aim to prevent the drainage of saltmarshes, with relevance to international carbon crediting projects and National GHG Inventories.

## 1 Introduction

Saltmarshes accumulate organic carbon (OC) of variable age and reactivity into their soils. A portion of this OC is stored for millennia, providing a climate regulation service, and some is returned to the atmosphere or laterally exported (Komada et al., 2022; Macreadie et al., 2021). Saltmarshes also accumulate and produce inorganic carbon (IC) but the climate regulation service of this is currently under debate and unclear (Granse et al., 2024; Van Dam et al., 2021).

To understand the role of saltmarsh soils in carbon cycling and their potential for climate mitigation through targeted management interventions, much research has focussed on determining the autochthonous (in-situ) and allochthonous (ex-situ, trapped during tidal inundation from terrestrial and marine sources) contributions to saltmarsh soils, with the accumulation of autochthonous OC as a direct sequestration of

carbon from the atmosphere, reducing the amount of atmospheric greenhouse gases (GHGs) (Macreadie et al., 2019; Saintilan et al., 2013; Van de Broek et al., 2018). The accumulation of allochthonous OC, originally sequestered outside the saltmarsh area, does not directly reduce atmospheric GHGs, but can represent a source of avoided emissions if it remains stored in the saltmarsh soil for longer than in an alternative depositional environment (Howard et al., 2023). Evidence to determine whether this is the case or not, and under what scenarios, has proven challenging to obtain (Gerald et al., 2019; Houston et al., 2024b). OC pools with distinct biological turnover times may instead provide greater insights into the soil carbon residence time and therefore the climate mitigation achieved through targeted management interventions to retain that carbon (Sanderman and Grandy, 2020).

Ramped oxidation (RO) and ramped pyrolysis oxidation (RPO) have been used to estimate the thermal reactivity and biological turnover time of soil and sediment OC (Hemingway et al., 2017b; Plante et al., 2011; Rosenheim et al., 2008). RO and RPO involve measuring the quantity of CO<sub>2</sub> evolved as a sample is increasingly heated at a constant rate in an atmosphere containing oxygen (e.g., Hemingway et al., 2017b; Plante et al., 2011; Stoner et al., 2023), or other gases, typically helium (e.g., Rosenheim et al., 2008). The temperature at which CO<sub>2</sub> is thermally-evolved is related to the activation energy required to thermally decompose C (Hemingway et al., 2017b), which is also an estimate of the energy required for biological degradation of OC (Peltre et al., 2013; Plante et al., 2013). CO<sub>2</sub> evolved at low temperatures is derived from soil OC pools with a greater thermal lability than CO<sub>2</sub> evolved at higher temperatures (Peltre et al., 2013; Rosenheim et al., 2008). OC thermal reactivity pools can be examined by collecting the evolved CO<sub>2</sub> from set temperature ranges with distinct thermal reactivities and measuring the <sup>14</sup>C (age) and <sup>13</sup>C content (Rosenheim et al., 2008), which can then be related to the activation energy required to thermally decompose those C sources (Hemingway et al., 2017b).

The <sup>14</sup>C content of the thermal reactivity pools provides insight into the turnover time of each pool, with past research showing that the oldest soil organic matter (OM) (most depleted <sup>14</sup>C content) tends to dominate the most thermally recalcitrant fractions (Bao et al., 2019b; Plante et al., 2013; Stoner et al., 2023). Similar results have been found for saltmarsh soils (Luk et al., 2021). Young OC, which can be autochthonous or allochthonous (Van de Broek et al., 2018), has been found to turnover at a faster rate than old OC in saltmarsh soils (Komada et al., 2022; Van de Broek et al., 2018), implying that young OC may tend to be more thermally labile than old OC for saltmarsh soils.

The <sup>13</sup>C content of the thermal reactivity pools can also provide insight as to whether the source of OC has an influence on turnover time. Previous work has found that the <sup>13</sup>C content of evolved CO<sub>2</sub> tends to be more enriched at higher temperatures due to greater contributions from <sup>13</sup>C-enriched,

degraded/microbially derived OC (Luk et al., 2021; Sanderman and Grandy, 2020; Stoner et al., 2023). Similarly, comparisons of the isotopic composition of thermally-defined OC pools to their chemical properties have found that thermally labile OC is derived from mostly lipids and polysaccharides, whereas OC with a higher thermal recalcitrance is derived from a greater proportion of phenolic and aromatic compounds (Sanderman and Grandy, 2020). The thermal reactivity of soil and sediment OC is also influenced by the formation of organo-mineral complexes, which can physically and chemically stabilise OC (Bianchi et al., 2024; Hemingway et al., 2019). Mineral-associations can increase the energy required for decomposition and have been found to increase thermal recalcitrance and to slow turnover times of soil and sediment OC (Hemingway et al., 2019; Stoner et al., 2023).

Crucially, the biological availability (bioavailability) of OC for decomposition, and hence its biological turnover time, is related to the prevailing environmental conditions as well as thermal reactivity (Hemingway et al., 2017b; Schmidt et al., 2011). For example, increased hydrodynamic energy can destabilise organo-mineral complexes and increase the bioavailability of previously stable OC (Spivak et al., 2019). Similarly, increased oxygen availability can decrease the energy requirement for microbes to decompose molecularly recalcitrant OC, causing it to be remineralised at a faster rate (Noyce et al., 2023).

Houston et al. (2024a) found that young OC stored in saltmarsh soils was preferentially respired as carbon dioxide (CO<sub>2</sub>) during aerobic incubation experiments, but that a portion of the respired CO<sub>2</sub> was produced from an aged (<sup>14</sup>C-depleted), allochthonous source. It is possible that this CO<sub>2</sub> could have been respired from thermally labile as well as thermally recalcitrant soil OC sources because the increased oxygen availability of the incubations potentially facilitated the degradation of OC which was previously stable in the low-oxygen environment of typical saltmarsh soils (Noyce et al., 2023).

The isotopic composition of RO thermal reactivity fractions can be compared to the isotopic composition of the CO<sub>2</sub> that is evolved biologically during incubations of equivalent samples to determine whether or not the age of the most biologically- and thermally-reactive OC pools match. Here, we present the first measurements of the <sup>13</sup>C and <sup>14</sup>C content of CO<sub>2</sub> derived from saltmarsh soils using RO, and the first comparison of these to the <sup>14</sup>C content of biologically evolved CO<sub>2</sub> from the same soils (Houston et al., 2024a). We hypothesised that the thermally labile C pools would be composed of younger C than the thermally recalcitrant pools, and that the CO<sub>2</sub> evolved from saltmarsh soils exposed to oxic conditions (Houston et al., 2024a) are from a predominantly thermally labile OC pool.

## 2 Methods

### 2.1 Field site and sample collection

Three saltmarsh soil cores (T1–3) were retrieved ca. 30 m apart from the lower marsh zone from Skinflats (SK), an estuarine saltmarsh in Scotland (56°3′34.04″ N, 3°43′59.16″ W), as detailed in Houston et al. (2024a). Field methods and laboratory sub-sampling procedures are described in detail in Houston et al. (2024a). Briefly, the cores were split into 1 cm thick slices as follows: core T1 (0–1, 5–6, and 18–19 cm); T2 (0–1, 5–6, and 15–16 cm), and T3 (0–1, 5–6, and 19–20 cm) (with the deepest sample from each core being the deepest retrieved sample from the 20 cm length of the corer. On the occasions when a full core was not retrieved, the deepest retrieved soil was used). Each slice was subsequently divided to provide sample material for the RO procedure, and for aerobic laboratory incubations from which the biologically evolved CO<sub>2</sub> was collected for <sup>13</sup>C and <sup>14</sup>C analysis (Houston et al., 2024a).

### 2.2 Ramped oxidation

The RO sub-samples were individually dried to constant mass before milling to a fine powder to homogenise and limit potential shielding effects from aggregates. Unlike most RO and RPO studies (e.g., Hemingway et al., 2017b), we did not remove carbonates from our samples. Acid treatment, which is required to remove carbonates from samples has been demonstrated to result in losses from the thermally labile OC fraction (Bao et al., 2019a), and affect the isotopic values of the lower temperature fractions (Rosengard et al., 2025). A loss of labile OC for our samples could seriously impact the interpretations in our study, and our ability to compare the <sup>14</sup>C content of the CO<sub>2</sub> respired from bulk (untreated) soils in the incubation experiments (Houston et al., 2024a) to the <sup>14</sup>C content of the RO thermal fractions.

The samples were sent to the NEIF Radiocarbon Laboratory for RO, which is described in Garnett et al. (2023). The RO procedure involved two stages, a first combustion to determine the relationship between the rate of CO<sub>2</sub> evolution and temperature (thermogram), and a second combustion where evolved sample gases were collected across defined temperature ranges, for subsequent isotope analysis. For the first combustion, ca. 200 mg of dried and homogenized sample material was weighed into a quartz vial which was inset into a quartz combustion tube, which was subsequently placed into a furnace set initially to room temperature. The furnace was progressively heated at a constant rate of 5 °C min<sup>−1</sup> to 800 °C in a stream of high purity oxygen (N5.5, BOC, UK). Heating caused combustion of the sample and the evolution of gas which was passed into a second quartz combustion tube containing platinised wool in a furnace set to a constant temperature of 950 °C. The platinised wool acted as a catalyst to ensure complete combustion of

the evolved gases. Upon exiting the secondary combustion chamber the sample passed through a glass tube containing magnesium perchlorate desiccant to remove moisture and subsequently the CO<sub>2</sub> concentration of the gas was measured using a non-dispersive infrared CO<sub>2</sub> sensor (SprintIR®-WF-5, Gas Sensing Solutions, UK). The sample was then passed out of the sensor unit and vented to the atmosphere.

The measured CO<sub>2</sub> concentration (normalised for sample mass) was plotted against temperature to produce thermograms which were used to identify temperature ranges, which defined C thermal reactivity pools for this study: 150–325, 325–425, 425–500, 500–650, and 650–800 °C.

For each sample, the required mass of material to evolve sufficient CO<sub>2</sub> (> 3 mL) for <sup>14</sup>C measurement was calculated based on the thermogram. A new sub-set from the original dried and homogenised sample was then re-run following the RO procedure outlined above, but instead of venting to atmosphere, after its measurement the evolved CO<sub>2</sub> was collected into foil gas bags based on the defined temperature ranges. CO<sub>2</sub> was collected for <sup>13</sup>C analysis from 650–800 °C, but sufficient CO<sub>2</sub> was evolved for <sup>14</sup>C analysis from this thermal fraction for only one sample (T1 0.5 cm, Table A1) and we do not consider this high temperature fraction further because it is likely dominated by carbonates and not relevant to the purpose of this study.

The foil gas bags (5 L Spout Pouch, <https://www.pouchshop.co.uk/>, last access: 20 October 2024) used for sample collection were sealed with one-hole rubber bungs into which a 0.6 cm diameter × 5 cm length stainless steel tube was inserted. Isoversinic tubing (Saint Gobain, France) was fitted over the stainless steel to connect it to a quick coupling (Colder Products Company, USA), which allowed connection to the RO kit.

Prior to the RO CO<sub>2</sub> collection, all equipment was cleaned using a standardised procedure (Garnett et al., 2023). All glassware was combusted at 900 °C for a minimum of 2 h, and all couplings and connectors were washed in carbon-free detergent (Decon) and rinsed in Milli-Q water. The foil gas bags were cleaned by repeatedly (3 times) filling with ca. 1 L high purity nitrogen gas (Research Grade 99.9995 % purity, BOC, UK) and evacuating with an air pump, over a period of at least 24 h (to aid out-gassing of CO<sub>2</sub>). The final evacuation, immediately before connecting to the RO rig, involved pumping out the bags with an SBA-5 CO<sub>2</sub> analyser (PPsystems, USA) to ensure that the bags did not contain significant contamination. Before commencing a sample combustion, the entire RO rig was checked for leaks and other potential sources of contamination by measuring the CO<sub>2</sub> concentration in the oxygen carrier gas exiting the kit, using the SBA-5 CO<sub>2</sub> analyser.

Within 3 d of combusting a sample, the evolved gas in each foil bag was connected to a vacuum rig for cryogenic recovery of pure sample CO<sub>2</sub> by passing it through slush (−78 °C; dry ice and industrial methylated spirits) and then liquid nitrogen (−196 °C) traps, under high vac-

uum (ca.  $3 \times 10^{-3}$  mbar). The sample  $\text{CO}_2$  was then split into three aliquots: One for  $\delta^{13}\text{C}$  analysis using isotope ratio mass spectrometry (IRMS; Delta V, Thermo-Fisher, Germany), one for graphitisation and subsequent AMS  $^{14}\text{C}$  analysis, and one for an archive back-up. The graphitised AMS samples were measured for  $^{14}\text{C}$  content at the SUERC AMS Laboratory (see Ascough et al., 2024). The  $^{13}\text{C}$  content ( $\delta^{13}\text{C}$ -VPDB) was used to normalise the  $^{14}\text{C}$  results to a  $\delta^{13}\text{C}$  of  $-25\text{‰}$  to correct for isotopic fractionation. Following convention,  $^{14}\text{C}$  results are presented as % Modern (fraction modern  $\times 100$ ) and conventional radiocarbon ages (years BP, where 0 BP = AD 1950 and age =  $-8033 \times \ln(\text{\%Modern} / 100)$ ).

### 2.3 Data Analysis

Continuous activation energy distributions ( $p(o, E)$ ) were modelled from thermograms using the “*rampedpyrox*” package in Python V3.8 (Hemingway, 2016; Hemingway et al., 2017b). For each temperature fraction which  $\text{CO}_2$  was collected from, the distributed activation energy model calculates mean activation energies ( $\mu\text{E}$ ) and the standard deviation of activation energy ( $\sigma\text{E}$ ), which is a measure of the heterogeneity of bond strength. Mean  $\mu\text{E}$ ,  $\sigma\text{E}$  and activation energy distribution ( $p(o, E)$ ) are also calculated for each sample using the model. Further data analysis and visualisation of thermograms and isotopic data was undertaken using RStudio V4.2.2 (R Core Team, 2022). Statistical analyses (ANOVAs for parametric data; Kruskal-Wallis for non-parametric data) were undertaken in Sigmaplot V12.5 (Systat Software Inc, 2013).

## 3 Results

### 3.1 Radiocarbon

The  $^{14}\text{C}$  content of the RO fractions (Fig. 1, Table 1) were statistically similar between the 0.5 cm, 5.5 cm, and deepest sample (T1 18.5 cm, T2 15.5 cm, T3 19.5 cm) depth increments for each of the temperature fractions (Kruskal-Wallis;  $p = 0.83, 0.38, 0.66, 0.99$ , for 150–325, 325–425, 425–500, 500–650 °C, respectively). There were, however, clear differences in  $^{14}\text{C}$  contents between the temperature fractions, with ranges of 81.50 %–97.54 % Modern for 150–325 °C, 41.67 %–79.80 % Modern for 325–425 °C, 17.67 %–63.56 % Modern for 425–500 °C, and 15.69 %–53.96 % Modern for 500–650 °C (Fig. 1, Table 1).

The RO samples were not pre-treated with acid, but the samples for bulk soil- $^{14}\text{C}$  were (Houston et al., 2024a), so we cannot verify that the weighted RO- $^{14}\text{C}$  contents amassed to the bulk soil  $^{14}\text{C}$  content. However, previous work using this analytical set-up have done this for other samples and shown that the combined RO fractions do equal the bulk isotope values (Garnett et al., 2023).

### 3.2 $\delta^{13}\text{C}$

There were no significant differences in the  $^{13}\text{C}$  content of the ramped oxidation fractions (Fig. 2, Table 2) between the depth increments (Kruskal-Wallis;  $p = 0.66, 0.63, 0.63, 0.44, 0.17$ , for 150–325, 325–400, 425–500, 500–650, 650–800 °C respectively).  $^{13}\text{C}$  contents followed the opposite trend to  $^{14}\text{C}$  contents with temperature, with ranges of  $-28.0\text{‰}$  to  $-24.7\text{‰}$  for 150–325 °C,  $-26.6\text{‰}$  to  $-22.3\text{‰}$  for 325–425 °C,  $-25.4\text{‰}$  to  $-20.2\text{‰}$  for 425–500 °C,  $-24.4\text{‰}$  to  $-13.9\text{‰}$  for 500–650 °C, and  $-21.1\text{‰}$  to  $-4.0\text{‰}$  for 650–800 °C (Fig. 2, Table 2).

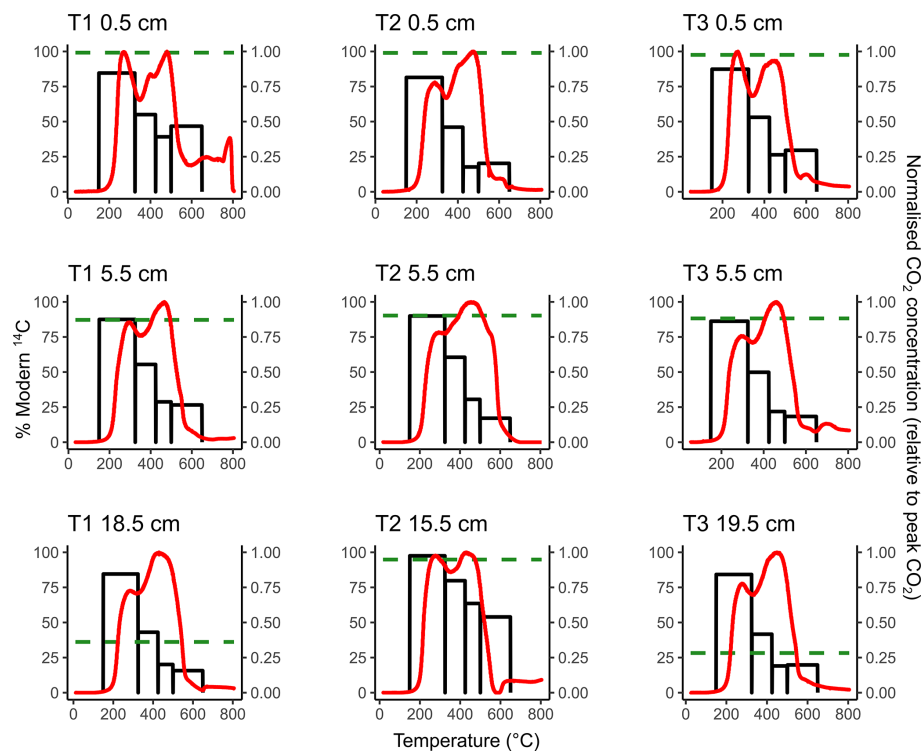
### 3.3 Ramped oxidation and incubation comparison

Figure 1 presents a comparison of the  $^{14}\text{C}$  content of the RO temperature fractions and respired  $\text{CO}_2$  from the same soils during aerobic laboratory incubations (Houston et al., 2024a). These comparisons show that for each of the 0.5 cm depth samples, the  $^{14}\text{C}$  content of the respired  $\text{CO}_2$  was greater than the  $^{14}\text{C}$  content of any of the RO temperature fractions in the same soils (Fig. 1). For the 5.5 cm depth samples, the  $^{14}\text{C}$  content of the  $\text{CO}_2$  respired in the incubations was approximately equivalent to the  $^{14}\text{C}$  content of the 150–325 °C RO temperature fraction (Fig. 1). For T2 15.5 cm, the  $^{14}\text{C}$  content of the respired  $\text{CO}_2$  was also closest to the 150–325 °C RO temperature fraction (Fig. 1). For the T1 18.5 cm and T3 19.5 cm samples, the  $^{14}\text{C}$  contents of the incubation  $\text{CO}_2$  were depleted relative to the 150–325 °C RO temperature fraction for both samples, and instead, were closest to the 325–425 °C and 425–500 °C RO temperature fractions, respectively (Fig. 1).

### 3.4 Activation Energy

$\mu\text{E}$  ranged from 157.50–170.97 kJ mol $^{-1}$  for the 0.5 cm depth samples, 159.97–165.32 kJ mol $^{-1}$  for the 5.5 cm depth samples, and 154.38–160.44 kJ mol $^{-1}$  for the deepest samples (T1 18.5 cm, T2 15.5 cm, T3 19.5 cm, Table 3).  $\sigma\text{E}$  ranged from 23.16–35.83 kJ mol $^{-1}$  for the 0.5 cm depth samples, 22.16–25.25 kJ mol $^{-1}$  for the 5.5 cm depth samples, and 21.43–23.51 kJ mol $^{-1}$  for the deepest samples (Table 3). Between the three depth increments, there were no significant changes in  $\mu\text{E}$  or  $\sigma\text{E}$  (Table 1; ANOVA;  $p = 0.47$  and  $0.37$ , respectively).

Table 4 shows  $\mu\text{fE}$  and the associated  $\sigma\text{fE}$  for each thermal fraction.  $\mu\text{fE}$  ranged from 131.04–133.23 kJ mol $^{-1}$  for 150–325 °C, 156.83–157.78 kJ mol $^{-1}$  for 325–425 °C, 176.14–177.79 kJ mol $^{-1}$  for 425–500 °C, 185.44–199.19 kJ mol $^{-1}$  for 500–650 °C, and 213.06–247.75 kJ mol $^{-1}$  for 650–800 °C (Table 4).  $\sigma\text{fE}$  ranged from 7.33–8.71 kJ mol $^{-1}$  for 150–325 °C, 9.83–10.23 kJ mol $^{-1}$  for 325–425 °C, 6.88–8.83 kJ mol $^{-1}$  for 425–500 °C, 3.68–16.04 kJ mol $^{-1}$  for 500–650 °C, and 1.83–10.94 kJ mol $^{-1}$  for 650–800 °C (Table 4).



**Figure 1.** Thermograms (red lines, right-hand y axis) overlaying the  $^{14}\text{C}$  content of ramped oxidation fractions (black bars, left-hand y axis) for each sample. The horizontal green dashed lines represent the  $^{14}\text{C}$  content of the  $\text{CO}_2$  respired from the aerobic incubation experiments of Houston et al. (2024a).

**Table 1.** Radiocarbon concentration (% Modern) of RO temperature fractions and the  $\text{CO}_2$  produced in soil incubation experiments in Houston et al. (2024a). Errors are reported to one standard deviation from the mean. A sole  $^{14}\text{C}$  measurement for T1 0.5 cm 650–800 °C is reported in Table A1.

	% Modern $^{14}\text{C}$				Incubation $\text{CO}_2$ (Houston et al., 2024a)
	150–325 °C	325–425 °C	425–500 °C	500–650 °C	
T1 0.5 cm	84.62 ± 0.44	55.02 ± 0.29	39.18 ± 0.21	46.75 ± 0.26	99.15 ± 0.45
T1 5.5 cm	87.51 ± 0.43	55.43 ± 0.28	28.76 ± 0.17	26.56 ± 0.16	87.18 ± 0.38
T1 18.5 cm	84.56 ± 0.44	43.06 ± 0.23	20.07 ± 0.13	15.70 ± 0.12	36.13 ± 0.36
T2 0.5 cm	81.50 ± 0.43	46.04 ± 0.24	17.67 ± 0.13	20.26 ± 0.14	98.97 ± 0.43
T2 5.5 cm	89.95 ± 0.42	60.55 ± 0.30	30.54 ± 0.17	17.11 ± 0.12	90.26 ± 0.40
T2 15.5 cm	97.53 ± 0.50	79.80 ± 0.41	63.56 ± 0.31	53.96 ± 0.27	94.86 ± 0.44
T3 0.5 cm	87.37 ± 0.45	53.09 ± 0.28	26.37 ± 0.15	29.55 ± 0.17	97.56 ± 0.43
T3 5.5 cm	86.23 ± 0.42	49.86 ± 0.25	21.87 ± 0.14	18.36 ± 0.12	88.22 ± 0.41
T3 19.5 cm	84.23 ± 0.41	41.67 ± 0.22	19.04 ± 0.13	19.76 ± 0.14	28.25 ± 0.37

$\mu\text{fE}$  and  $\sigma\text{fE}$  both varied significantly between the thermal fractions, increasing sequentially (Kruskal-Wallis,  $p = 0.001$  and  $0.001$ , respectively).

4 Discussion

Soils are complex mixtures of many different OC sources and ages, with different vulnerabilities to decomposition and turnover. In this study, we aimed to improve our understanding of the carbon cycling of saltmarsh soils by measuring the  $^{13}\text{C}$  and  $^{14}\text{C}$  content of thermally-fractionated soil carbon pools, and comparing these results to the  $^{14}\text{C}$  content of

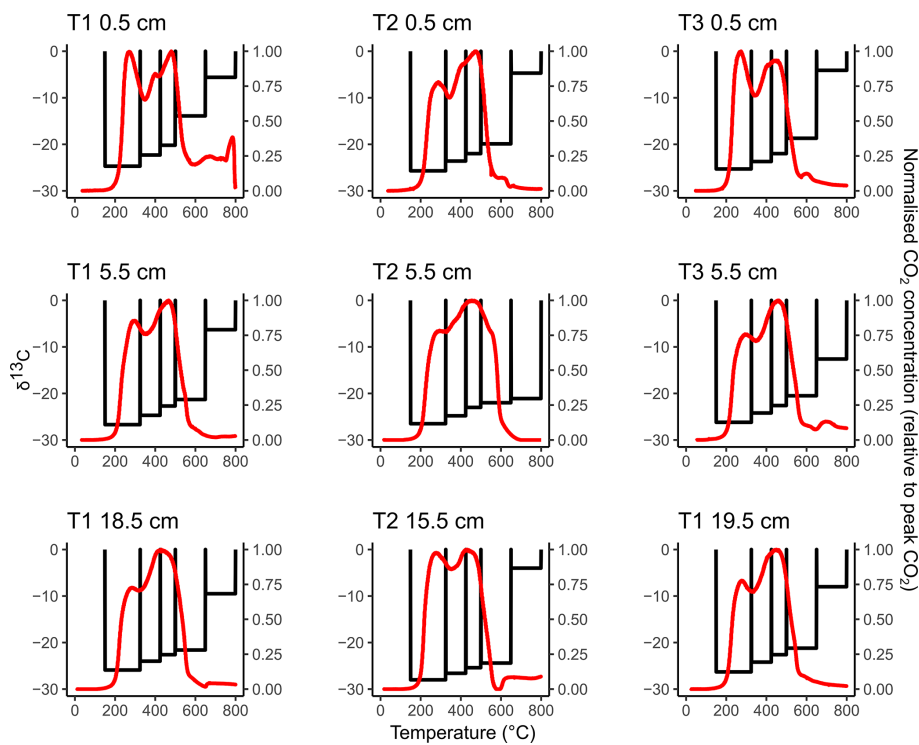


**Figure 2.** Thermograms (red lines, right-hand y axis) overlaying the  $^{13}\text{C}$  content of the RO temperature fractions (black bars, left-hand y axis) for each sample. Unlike Fig. 1, we did not attempt to relate the  $^{13}\text{C}$ -RO to the  $^{13}\text{C}$  content of the  $\text{CO}_2$  respired in the incubation experiments, due to the potential for microbial fractionation during the incubation experiments.

**Table 2.**  $\delta^{13}\text{C}$ -VPDB ‰ signature of the RO temperature fractions and the incubation experiments in Houston et al. (2024a). Errors are reported to one standard deviation from the mean.

	$\delta^{13}\text{C}$ -VPDB ‰					Incubations (Houston et al., 2024a)
	150–325 °C	325–425 °C	425–500 °C	500–650 °C	650–800 °C	
T1 0.5 cm	$-24.7 \pm 0.1$	$-22.3 \pm 0.1$	$-20.2 \pm 0.1$	$-13.9 \pm 0.1$	$-5.6 \pm 0.1$	$-23.3 \pm 0.1$
T1 5.5 cm	$-26.7 \pm 0.1$	$-24.7 \pm 0.1$	$-22.7 \pm 0.1$	$-21.3 \pm 0.1$	$-6.3 \pm 0.1$	$-23.6 \pm 0.1$
T1 18.5 cm	$-25.9 \pm 0.1$	$-24.0 \pm 0.1$	$-22.6 \pm 0.1$	$-21.6 \pm 0.1$	$-9.5 \pm 0.1$	$-6.1 \pm 0.1$
T2 0.5 cm	$-25.7 \pm 0.1$	$-23.6 \pm 0.1$	$-22.0 \pm 0.1$	$-19.9 \pm 0.1$	$-4.7 \pm 0.1$	$-22.9 \pm 0.1$
T2 5.5 cm	$-26.5 \pm 0.1$	$-24.8 \pm 0.1$	$-23.0 \pm 0.1$	$-22.0 \pm 0.1$	$-21.1 \pm 0.1$	$-23.1 \pm 0.1$
T2 15.5 cm	$-28.0 \pm 0.1$	$-26.6 \pm 0.1$	$-25.4 \pm 0.1$	$-24.4 \pm 0.1$	$-4.0 \pm 0.1$	$-20.2 \pm 0.1$
T3 0.5 cm	$-25.3 \pm 0.1$	$-23.7 \pm 0.1$	$-22.0 \pm 0.1$	$-18.7 \pm 0.1$	$-4.1 \pm 0.1$	$-20.6 \pm 0.1$
T3 5.5 cm	$-26.2 \pm 0.1$	$-24.2 \pm 0.1$	$-22.6 \pm 0.1$	$-20.5 \pm 0.1$	$-12.6 \pm 0.1$	$-23.4 \pm 0.1$
T3 19.5 cm	$-26.3 \pm 0.1$	$-24.2 \pm 0.1$	$-22.6 \pm 0.1$	$-21.2 \pm 0.1$	$-8.0 \pm 0.1$	$-3.7 \pm 0.1$

biologically evolved  $\text{CO}_2$  from the same soils (Houston et al., 2024a).

4.1 Carbon provenance of ramped oxidation  $\text{CO}_2$  fractions

The first three RO temperature fractions (150–325, 325–425, 425–500 °C) were derived solely from OC sources, as IC begins to breakdown from ca. 550 °C (Hemingway et al., 2017b).  $\text{CO}_2$  from the 500–650 and 650–800 °C fractions

may, however, have been evolved from a mix of OC and IC sources. The IC contents of the studied soils (0.11 %–0.48 %) were low relative to OC contents (4.18 %–7.71 %), and IC makes only 1.95 %–10.48 % of the total soil C pool for these samples (Table A2).

IC could have been removed from our saltmarsh soil samples to allow complete analysis of the soil OC pool, and many R(P)O studies have taken this approach (Bao et al., 2019b; Hemingway et al., 2017b; Luk et al., 2021; Stoner et al.,

**Table 3.**  $\mu\text{E}$  and  $\sigma\text{E}$  for each sample.

	$\mu\text{E}$ ( $\text{kJ mol}^{-1}$ )	$\sigma\text{E}$ ( $\text{kJ mol}^{-1}$ )
T1 0.5 cm	170.97	35.83
T1 5.5 cm	159.97	22.16
T1 18.5 cm	160.44	22.72
T2 0.5 cm	160.47	23.16
T2 5.5 cm	165.32	25.25
T2 15.5 cm	154.38	21.43
T3 0.5 cm	157.50	24.01
T3 5.5 cm	162.31	24.44
T3 19.5 cm	160.13	23.51

2023; Williams and Rosenheim, 2015). However, our samples have low IC contents (Table A2), and acid-treatment, which is required to remove IC from samples, can cause losses of labile OC (Bao et al., 2019a). Indeed, in Hemingway et al. (2017b), acid treatment of samples prior to RO resulted in a shift of 4 % Modern  $^{14}\text{C}$ , which could change one of our samples from having a pre-bomb  $^{14}\text{C}$  content to a post-bomb  $^{14}\text{C}$  content, or vice-versa. A similar shift in  $^{14}\text{C}$  content for our samples could seriously impact the interpretations in our study, and our ability to compare the  $^{14}\text{C}$  content of the  $\text{CO}_2$  respired from bulk (untreated) soils in the incubation experiments (Houston et al., 2024a) to the  $^{14}\text{C}$  content of the RO fractions. The soils in the incubation experiments were also not decarbonated as the acid-treatment would have affected soil respiration processes and made the results incomparable to in-situ soil degradation processes (Houston et al., 2024a).

#### 4.2 $^{14}\text{C}$ content of ramped oxidation $\text{CO}_2$ fractions

The  $^{14}\text{C}$ -RO content decreased over the four thermal fractions (150–325, 325–425, 425–500, 500–650 °C, Fig. 1), implying that  $^{14}\text{C}$ -depleted OC had a greater thermal recalcitrance than  $^{14}\text{C}$ -enriched OC for these saltmarsh soil samples. Since the  $^{14}\text{C}$  content of each RO fraction was < 100 % Modern (Table 1), each of the OC reactivity pools were likely to be predominantly composed of carbon sequestered from the atmosphere before the 1963  $^{14}\text{C}$  bomb-spike caused by atmospheric nuclear weapons testing, although we cannot completely discount some contributions from post-bomb carbon (Hajdas et al., 2021). Nevertheless, using  $^{14}\text{C}$  content as an estimate of the age of the OC we can infer that the older ( $^{14}\text{C}$ -depleted) OC has a greater thermal recalcitrance than young OC for these samples, which is consistent with previous studies on the thermal reactivity of carbon stored in soils and sediments (e.g., Bao et al., 2019b; Luk et al., 2021; Plante et al., 2013; Stoner et al., 2023).

The results suggest inhomogeneity within at least one of the temperature fractions for each sample because, while there were no post-bomb  $^{14}\text{C}$  contents for the incubation or RO samples (Table 1), there is likely to be a fraction of

post-bomb (post-AD1955) OC in at least one of the temperature fractions. Autochthonous OC sequestration (post-bomb) at this accreting saltmarsh (Hajdas et al., 2021; Smeaton et al., 2024) may become obscured by contributions from pre-bomb (pre-AD1955) OC. Observing the decline in  $^{14}\text{C}$  content with increasing temperature (Fig. 1), we hypothesise that, if present, this mixing of pre- and post-bomb C most likely occurred in the 150–325 °C fraction.

As the oldest (most  $^{14}\text{C}$ -depleted) C had the greatest thermal recalcitrance (Fig. 1), this emphasises that saltmarshes accumulating greater amounts of older ( $^{14}\text{C}$ -depleted) OC will likely provide the most thermally recalcitrant OC stores, and saltmarshes accumulating greater proportions of contemporary OC, either through in-situ production or young allochthonous components, contain soil OC stores which are of greater thermal lability (Komada et al., 2022; Van de Broek et al., 2018). However, the  $^{14}\text{C}$  contents of the lowest temperature RO fraction (81 %–98 % Modern; Table 1) highlight that although  $^{14}\text{C}$  content decreases with decreasing thermal reactivity (Fig. 1), thermally labile OC can still be aged (at least hundreds of years old) for these soils. Due to the often anaerobic and non-eroding conditions of buried sediments, saltmarshes can therefore be stores of old, but thermally labile carbon. Of course, the thermal recalcitrance of OC is not necessarily related to biological turnover time, as this is also related to the prevailing environmental conditions (Schmidt et al., 2011; Spivak et al., 2019).

#### 4.3 $^{13}\text{C}$ content of ramped oxidation $\text{CO}_2$ fractions

$^{13}\text{C}$ -RO increased sequentially with the thermal fractions (Fig. 2), due to greater contributions from relatively  $^{13}\text{C}$ -enriched C sources from the higher temperature thermal fractions. The  $^{13}\text{C}$ -RO contents of the 150–650 °C fractions were each typical of OC sources (Leng and Lewis, 2017), whereas the  $^{13}\text{C}$ -RO contents of the 650–800 °C fraction were mostly typical of at least a partial contribution from an IC source, with the exception of T2 5.5 cm and T3 5.5 cm (Table 2) (Brand et al., 2014; Ramnarine et al., 2012). As IC can begin to evolve from 550 °C, it is possible that a mix of OC and IC sources was present in the 500–650 °C thermal fractions.

As  $^{13}\text{C}$ -RO increased with temperature (Fig. 2, Table 2),  $^{13}\text{C}$ -enriched OC had a greater thermal recalcitrance than  $^{13}\text{C}$ -depleted OC for these samples. Previous work has demonstrated that > 80 % of the OC accumulating at Skinflats saltmarsh is autochthonous/terrestrial in origin (Miller et al., 2023), with limited contributions from marine OC. The thermally recalcitrant OC was potentially composed of a greater amount of OC which has undergone microbial decomposition as this process tends to enrich the degraded OC in  $^{13}\text{C}$  (Boström et al., 2007; Etcheverría et al., 2009; Luk et al., 2021; Sanderman and Grandy, 2020; Soldatova et al., 2024; Stoner et al., 2023). The thermally recalcitrant OC may instead/also have been composed of different OM compounds (e.g., lignins, aromatics) than the more thermally la-

**Table 4.**  $\mu$ fE and  $\sigma$ fE for each RO temperature fraction for each sample.

	$\mu$ fE ( $\sigma$ fE) (kJ mol <sup>−1</sup> )				
	150–325 °C	325–425 °C	425–500 °C	500–650 °C	650–800 °C
T1 0.5 cm	132.43 (7.33)	157.52 (10.17)	177.79 (7.32)	199.19 (16.04)	242.42 (10.94)
T1 5.5 cm	133.23 (8.07)	157.00 (10.13)	177.07 (7.58)	191.06 (7.87)	213.06 (2.12)
T1 18.5 cm	131.90 (8.62)	157.60 (9.83)	176.93 (7.83)	189.53 (6.70)	239.73 (6.73)
T2 0.5 cm	132.10 (8.21)	157.42 (10.08)	177.23 (7.38)	191.39 (10.62)	226.84 (6.81)
T2 5.5 cm	132.15 (8.71)	157.11 (10.01)	177.68 (8.83)	195.80 (7.95)	224.56 (4.55)
T2 15.5 cm	131.04 (8.46)	156.83 (10.23)	176.69 (6.88)	185.44 (3.68)	247.74 (1.83)
T3 0.5 cm	131.59 (7.48)	157.33 (10.07)	176.14 (7.07)	193.65 (12.46)	231.21 (10.04)
T3 5.5 cm	133.05 (8.28)	157.67 (10.14)	177.19 (7.70)	191.13 (9.11)	236.57 (4.29)
T3 19.5 cm	131.73 (8.38)	157.78 (10.00)	176.71 (7.34)	191.7 (10.53)	232.23 (9.69)

bile OC (e.g., carbohydrates, lipids) (Sanderman and Grandy, 2020). It is also possible that methodological artefacts, such as kinetic fractionation, influenced the <sup>13</sup>C-RO contents. Kinetic fractionation is explained by different carbon isotopes evolving as CO<sub>2</sub> from the soil sample at different rates during the ramped heating (Hemingway et al., 2017a). Kinetic fractionation would cause the <sup>13</sup>C content of the evolved CO<sub>2</sub> to increase linearly with temperature (Hemingway et al., 2017a), and we cannot rule out this artefact. Hemingway et al. (2017a) determined that kinetic fractionation was not an important factor in their RPO procedure, but we used a different set-up (described in Garnett et al., 2023).

**4.4 Changes in the isotopic content of ramped oxidation CO<sub>2</sub> fractions with depth**

The isotopic composition of the evolved CO<sub>2</sub> did not vary significantly with depth for any of the temperature fractions. The lack of an increase in the age (<sup>14</sup>C-depletion) of soil C with sample depth is unusual, as typically C undergoes a burial process, and previous work has shown diagenetic ageing of saltmarsh soils with depth as young OC is turned over faster than old OC (Komada et al., 2022; Van de Broek et al., 2018).

Compared to other UK saltmarshes, Skinflats has relatively high C accumulation rates (Miller et al., 2023; Smeaton et al., 2024). Depleted <sup>14</sup>C contents of the OC accumulating at the Skinflats saltmarsh (Houston et al., 2024a) imply that a proportion of the OC being buried may already have been aged at the time of deposition on the marsh surface, as the marsh formed in the 1930s (Miller et al., 2023). The combination of high carbon accumulation rates and depleted soil <sup>14</sup>C contents implies that the Skinflats saltmarsh accumulates a high proportion of old, most likely allochthonous OC. Some of the aged, allochthonous OC may have undergone significant microbial processing and degradation prior to its accumulation in the saltmarsh soil. As the OM is degraded, and the energetically favourable components are consumed, the resulting OM becomes increasingly thermally recalcitrant (Luk et al., 2021; Sanderman and

Grandy, 2020; Soldatova et al., 2024). The accumulation of a high proportion of degraded OC on the Skinflats saltmarsh may therefore explain the lack of observed change in the isotopic composition of the soil OC pools with depth. This interpretation is supported by the lack of change in both the amount and the proportion of CO<sub>2</sub> evolved from each temperature fraction with depth (ANOVAs, *p* > 0.05; Table A3).

Not all old OC is degraded or thermally recalcitrant, and our results show that the Skinflats saltmarsh is also a store of old (<sup>14</sup>C-depleted), thermally labile OC (Fig. 1). Old OC can be thermally labile if it “ages” (is stored) in an environment with low decomposition rates, e.g., a peatland (Dean et al., 2023), prior to transport and accumulation into the saltmarsh. There are extensive peatlands in the Skinflats catchment, many of which are degrading (Lilly et al., 2012). Regardless of the age and degradation state of the OC deposited onto the marsh surface, as it gets buried it will undergo a degree of microbial processing and degradation in the saltmarsh soil (Luk et al., 2021), but that process is potentially less prevalent at Skinflats than saltmarshes accumulating younger, less degraded OC.

Through isotopic analysis of saltmarsh soils partitioned using ramped oxidation, we have determined that increased thermal recalcitrance is related to older (<sup>14</sup>C-depleted; Fig. 1), more degraded/microbially derived (<sup>13</sup>C-enriched; Fig. 2) soil C. These findings are consistent with previous research on the thermal reactivity of soil and sediment C, which have found that in most cases, more energy is required (higher temperature/ $\mu$ fE) to decompose older (<sup>14</sup>C-depleted), degraded/microbially derived (<sup>13</sup>C-enriched) C than younger (<sup>14</sup>C-enriched), less processed (<sup>13</sup>C-depleted) C (e.g., Bao et al., 2019b; Plante et al., 2013; Stoner et al., 2023), including one saltmarsh study (Luk et al., 2021).

**4.5 Comparison of biologically and thermally evolved CO<sub>2</sub>**

As the biological turnover time of OC is related to the prevailing environmental conditions as well as thermal reactivity, the isotopic composition of the most biologically- and



thermally-reactive saltmarsh soil OC pools may not be the same. To determine if this is the case, or not, we compared the isotopic composition of the RO thermal reactivity fractions to the isotopic composition of the CO<sub>2</sub> that was evolved biologically during incubations of equivalent samples (Houston et al., 2024a) (Fig. 1).

Figure 1 shows that for each of the 0.5 cm depth samples, the <sup>14</sup>C content of the CO<sub>2</sub> respired in the aerobic laboratory experiments was <sup>14</sup>C-enriched relative to any of the RO temperature fractions, which was also the case for the T3 5.5 cm sample (Table 3). The relative <sup>14</sup>C-enrichment of the biologically respired CO<sub>2</sub> compared to the thermally evolved CO<sub>2</sub> was likely caused by inhomogeneity in the OC thermal reactivity pools, as each defined thermal reactivity pool may be composed of multiple OC sources of variable age and composition. As thermal recalcitrance is related to <sup>14</sup>C-depletion for these samples (Fig. 1), we hypothesise that for saltmarsh soil samples producing respired CO<sub>2</sub> that was <sup>14</sup>C-enriched relative to any of the RO fractions (T1 0.5 cm, T2 0.5 cm, T3 0.5 cm, T3 5.5 cm; Table 1, Fig. 1), that this CO<sub>2</sub> was biologically-produced from an OC pool within the most thermally labile RO fraction (150–325 °C). Thus, we suggest that even within the 150–325 °C RO fraction there are pools of even younger OC, but that they are masked by older, <sup>14</sup>C-depleted OC. Similar findings of mixing within thermal fractions has been reported in previous RPO work (e.g., Rosen-gard et al., 2025; Rosenheim et al., 2008).

The <sup>14</sup>C content of respired CO<sub>2</sub> from the 5.5 cm depth samples tended to be closer to the <sup>14</sup>C content of the lowest temperature (150–325 °C) RO fraction (Fig. 1), implying that for these samples the biologically evolved CO<sub>2</sub> was from a thermally labile OC pool. The T2 15.5 cm respired CO<sub>2</sub> sample was also similar in <sup>14</sup>C content to the lowest temperature RO fraction, whereas respired CO<sub>2</sub> from the slightly deeper T1 18.5 cm and T3 19.5 cm samples was <sup>14</sup>C-depleted relative to the 150–325 °C RO fraction, instead aligning closer to the higher temperature RO fractions (Fig. 1). The biologically evolved CO<sub>2</sub> from T1 18.5 cm and T3 19.5 cm were therefore potentially derived from less thermally labile OC pools than the other samples, although it is possible that the thermally labile pools were composed of multiple OC sources with different <sup>14</sup>C contents. The <sup>14</sup>C content of the CO<sub>2</sub> evolved from the aerobic incubations of T1 18.5 cm and T3 19.5 cm was hypothesized to have been derived from an inorganic C source due to the enriched <sup>13</sup>C contents of −6.1 ‰ and −3.7 ‰, respectively (Houston et al., 2024a). As IC biological turnover times are controlled by different factors than OC (Van Dam et al., 2021), and the remainder of the samples were determined to evolve from OC substrates, this is likely to explain why the <sup>14</sup>C content of the CO<sub>2</sub> evolved from the aerobic incubation experiments for T1 18.5 cm and T3 19.5 cm did not align with the lowest temperature (most thermally labile) RO fraction (Fig. 1). Therefore, there was a clear depth trend in the relationship between the <sup>14</sup>C content of CO<sub>2</sub> respired in the aerobic incubation ex-

periments and the <sup>14</sup>C content of RO fractions of the same bulk soils. Degradation of some of the thermally labile OM components during burial may reduce the range of differently aged OC sources within the most thermally labile RO fraction for the deeper samples in this study.

For seven out of nine samples (T1 18.5 cm and T3 19.5 cm being the outliers), the <sup>14</sup>C content of the CO<sub>2</sub> evolved from the aerobic laboratory incubations was closest to the <sup>14</sup>C content of the 150–325 °C RO temperature fraction. Therefore, even though the CO<sub>2</sub> evolved from the aerobic incubation experiments was determined to be from a predominantly aged, allochthonous OC source (Houston et al., 2024a), it can now also be shown to be derived from a predominantly thermally labile OC pool (Fig. 1).

We did not attempt to relate the <sup>13</sup>C-RO to the <sup>13</sup>C content of the CO<sub>2</sub> respired in the incubation experiments, due to the potential for microbial fractionation during the incubation experiments which can change the <sup>13</sup>C content of the respired CO<sub>2</sub> and the resulting soil OC (Soldatova et al., 2024; Werth and Kuzyakov, 2010). In contrast, <sup>14</sup>C results are normalised using the measured  $\delta^{13}\text{C}$  values and are therefore immune to such isotopic fractionation effects.

#### 4.6 Implications

Our results show that aged (presumed allochthonous), thermally labile OC stored in saltmarsh soils remains vulnerable to loss to the atmosphere upon habitat drainage. Saltmarsh soils usually exist in low-oxygen, tidally-inundated conditions which slow decomposition of OC (Chapman et al., 2019), but many saltmarshes globally have been drained (and their soils subsequently oxidised) to convert them for land uses such as housing developments and agriculture (Bromberg and Bertness, 2005; Campbell et al., 2022; Morris et al., 2012). In the Forth Estuary, where the Skinflats saltmarsh is located, as much as 50 % of the intertidal area has been converted to agricultural land since 1600, often involving the drainage of saltmarshes (Hansom and McGlashan, 2004).

Protecting saltmarshes from degradation following drainage is listed as an eligible activity for generating carbon credits for blue carbon ecosystem (BCE) projects (VERRA, 2023) and there is significant potential for climate mitigation by avoided emissions from protecting vulnerable stocks of soil OC in BCEs (Goldstein et al., 2020; Griscom et al., 2017; Kwan et al., 2025; Sasmito et al., 2025). Similarly, the re-creation of saltmarsh habitat through managed realignment (rewetting by tidal inundation) of historic saltmarsh habitats which were previously reclaimed for land use purposes (e.g., agriculture) could reduce (and possibly reverse) the emissions of aged OC to the atmosphere, both locally to Skinflats, and globally.

The evidence for the respiration of thermally labile, allochthonous OC from saltmarsh soils in a drainage degradation scenario demonstrates that at least this fraction of

allochthonous OC could be counted as additional in carbon crediting projects and National GHG Inventories. Because allochthonous OC can account for up to 90 % of saltmarsh soil carbon (Komada et al., 2022), the inclusion of allochthonous OC (or even a fraction of it) would significantly increase the climate mitigation awarded to blue carbon projects (as carbon credits, or contributions to National GHG Inventories) (Houston et al., 2024b).

As the bioavailable OC respired in the experiments of Houston et al. (2024a) was (in most cases) from a predominantly thermally labile OC pool, and  $^{14}\text{C}$ -RO decreased (C became older) with increasing temperature (thermal recalcitrance), RO measurements could be useful for characterising the turnover times of OC pools for saltmarsh soils exposed to oxic conditions (drainage degradation scenario). The use of thermally defined OC pools to characterize OC turnover times for saltmarsh soils would require a modelling advancement to constrain degradation rates and residence times. Such efforts are not within the scope of this study but could inform additionality/permanence in these saltmarsh systems. Experimentally defined turnover times of OC thermal reactivity pools could, for example, provide a more robust approach than inclusion/exclusion of allochthonous OC from saltmarsh “blue carbon” projects (Houston et al., 2024b).

Further research is needed to determine if the relationship between biological and thermal lability exists for different degradation scenarios such as nutrient enrichment, as OC turnover time is related to the environmental conditions as well as the thermal lability of the OC pools. Similarly, these experiments would need to be replicated for a wider range of saltmarshes (high and low latitude saltmarshes, different typologies), as there are likely to be differences in OC turnover in different systems.

The samples used for this study were from the low marsh zone only, but it is likely that the thermal reactivity of the Skinflats saltmarsh soil C will vary spatially across the marsh, as the proportion of OC sources has been shown to be variable across saltmarshes (Middelburg et al., 1997). Given our findings that old ( $^{14}\text{C}$ -depleted) OC has greater thermal recalcitrance than young ( $^{14}\text{C}$ -enriched) OC (Fig. 1), we anticipate that higher marsh zones, which typically have greater proportions of autochthonous OC than lower marsh zones (Spohn et al., 2013), would contain a greater proportion of thermally labile OC. However, it is important to recognise that some of the young ( $^{14}\text{C}$ -enriched), autochthonous OC in saltmarsh soils can also be thermally recalcitrant. As well as marsh zonation, we expect that the proportion of OC sources (and associated mix of thermal reactivities) would also vary with proximity to marsh creeks which redistribute autochthonous and allochthonous C across the saltmarsh habitat (Middelburg et al., 1997; Reed et al., 1999). In previously published work we showed that Skinflats accumulates OC of a much greater “age” (depleted soil  $^{14}\text{C}$  contents) than two other saltmarshes in Scotland (Houston et al., 2024a).

In this paper we have determined that age ( $^{14}\text{C}$ -content) is related to the thermal recalcitrance of saltmarsh soil OC. We therefore speculate that sites accumulating younger OC would have more thermally labile soil OC than sites accumulating older OC, like Skinflats, with wider implications for the risks to these vulnerable stores of soil carbon from human disturbances.

5 Conclusions

This is the first study on saltmarsh soils to employ the ramped oxidation method. We show that old ( $^{14}\text{C}$ -depleted) carbon dominates the thermally recalcitrant OC pools. The thermally labile OC pools are also aged ( $^{14}\text{C}$ -depleted) compared to the contemporary atmosphere but are younger than the thermally recalcitrant OC pools. These results highlight the role of saltmarshes as mixed stores of both old, thermally recalcitrant OC, as well as younger, thermally labile OC.

We present the first comparison of the bioavailability ( $\text{CO}_2$  evolved from incubation experiments; Houston et al., 2024a) and the thermal reactivity (RO) of saltmarsh soil OC. We show that aged, allochthonous  $\text{CO}_2$  evolved from saltmarsh soils exposed to oxic conditions (Houston et al., 2024a) are from a predominantly thermally labile OC pool. As saltmarsh soils exist mostly in low oxygen, waterlogged conditions, management interventions to limit their exposure to elevated oxygen availability may protect and conserve these stores of thermally labile OC and provide a climate abatement service. Therefore, we recommend that thermally labile allochthonous OC stored in saltmarsh soils should be counted as additional in some carbon crediting projects and National GHG Inventories.

Appendix A

**Table A1.** Additional  $^{14}\text{C}$  measurement from the 650–800 °C.  $^{14}\text{C}$  was measured at the Scottish Universities Environmental Research Centre Accelerator Mass Spectrometer (AMS) Laboratory.  $\delta^{13}\text{C}$  (relative to Vienna PDB standard) was measured using isotope ratio mass spectrometry on a Delta V (Thermo, Germany) and used to normalize the  $^{14}\text{C}$  results to a  $\delta^{13}\text{C} = -25\text{‰}$ , which were reported as % Modern  $^{14}\text{C}$  (i.e., Fraction modern  $\times 100$ ). Errors are reported to one standard deviation from the mean.

Sample ID	% Modern $^{14}\text{C}$
Skin T1 0.5 cm 650–800 °C	$79.75 \pm 0.50$

**Table A2.** Soil carbon properties measured on equivalent sub-samples prior to the RO procedure, as reported in Houston et al. (2024a). Total organic carbon (TOC), Total carbon (TC) for the soil samples were measured by a SoliTOC analyser (Elementar Analysensysteme, Hanau, Germany).  $^{14}\text{C}$  was measured at the Scottish Universities Environmental Research Centre Accelerator Mass Spectrometer (AMS) Laboratory.  $\delta^{13}\text{C}$  (relative to Vienna PDB standard) was measured using isotope ratio mass spectrometry on a Delta V (Thermo, Germany) and used to normalize the  $^{14}\text{C}$  results to a  $\delta^{13}\text{C} = -25\text{‰}$ , which were reported as % Modern  $^{14}\text{C}$  (i.e., Fraction modern  $\times 100$ ). Errors are reported to one standard deviation from the mean.

Sample ID	TOC (%)	TIC (%)	TC (%)	% Modern $^{14}\text{C}$	$\delta^{13}\text{C}$
SK T1 0.5 cm	4.1	0.48	4.58	$47.49 \pm 0.23$	$-23.5 \pm 0.1$
SK T1 5.5 cm	4.96	0.11	5.06	$45.03 \pm 0.20$	$-24.5 \pm 0.1$
SK T1 18.5 cm	4.8	0.39	5.18	$41.36 \pm 0.19$	$-23.8 \pm 0.1$
SK T2 0.5 cm	4.71	0.16	4.87	$31.47 \pm 0.15$	$-22.2 \pm 0.1$
SK T2 5.5 cm	4.23	0.13	4.36	$43.69 \pm 0.21$	$-24.1 \pm 0.1$
SK T2 15.5 cm	7.56	0.15	7.71	$50.93 \pm 0.24$	$-25.1 \pm 0.1$
SK T3 0.5 cm	5.37	0.12	5.49	$47.03 \pm 0.22$	$-23.7 \pm 0.1$
SK T3 5.5 cm	4.06	0.11	4.18	$44.15 \pm 0.21$	$-24.0 \pm 0.1$
SK T3 19.5 cm	5.23	0.12	5.35	$44.48 \pm 0.21$	$-24.1 \pm 0.1$

**Table A3.** Percentage (%) carbon evolved for each RO temperature fraction for each sample, and the relative contribution (%) to the total C evolved over the  $\text{CO}_2$  collection temperature interval (150–650 °C).

	% Carbon (% of Total Evolved $\text{CO}_2$ )				
	150–325 °C	325–425 °C	425–500 °C	500–650 °C	150–650 °C
T1 0.5 cm	1.42 (34.64)	1.17 (26.90)	1.07 (24.60)	0.69 (15.86)	4.35
T1 5.5 cm	1.44 (29.94)	1.59 (33.06)	1.11 (23.08)	0.67 (13.93)	4.81
T1 19.5 cm	1.48 (3.58)	1.43 (29.55)	1.31 (27.07)	0.62 (12.81)	4.84
T2 0.5 cm	1.45 (30.33)	1.30 (27.20)	1.44 (30.13)	0.59 (12.34)	4.78
T2 5.5 cm	1.09 (24.55)	1.13 (25.45)	1.12 (25.23)	1.1 (24.77)	4.44
T2 15.5 cm	2.66 (32.40)	2.60 (31.67)	2.12 (25.82)	0.83 (10.11)	8.21
T3 0.5 cm	1.98 (35.93)	1.6 (29.04)	1.38 (25.05)	0.55 (9.98)	5.51
T3 5.5 cm	1.13 (27.49)	1.32 (32.12)	1.08 (26.28)	0.58 (14.11)	4.11
T3 19.5 cm	1.48 (29.72)	1.75 (35.14)	1.11 (22.29)	0.64 (12.85)	4.98

**Data availability.** All data presented in this manuscript is available in the main text and Appendix tables.

**Supplement.** The supplement related to this article is available online at <https://doi.org/10.5194/bg-22-4851-2025-supplement>.

**Author contributions.** AH undertook the study, fieldwork, sample processing, data acquisition, and wrote the first draft of the manuscript. MHG conducted the laboratory procedures with the help of AH, AH, WENA, and MHG contributed to designing the study, fieldwork, and laboratory analyses. WENA and MHG oversaw the study and contributed to writing and revision of the manuscript.

**Competing interests.** The contact author has declared that none of the authors has any competing interests.

**Disclaimer.** Publisher's note: Copernicus Publications remains neutral with regard to jurisdictional claims made in the text, published maps, institutional affiliations, or any other geographical representation in this paper. While Copernicus Publications makes every effort to include appropriate place names, the final responsibility lies with the authors. Also, please note that this paper has not received English language copy-editing. Views expressed in the text are those of the authors and do not necessarily reflect the views of the publisher.

**Acknowledgements.** We thank Jo Smith (University of Aberdeen) for her comments and edits on the first draft of this manuscript. Thanks are extended to Chloe Bates for assisting with sample collection. Finally, we thank the editor and both reviewers for their comments which have improved this manuscript.

**Financial support.** This research has been supported by UK Research and Innovation grant nos. NE/S007342/1 and

NE/S011587/1, NEIF Radiocarbon allocation nos. 2594.1022 and 2709.1023, and EU HORIZON EUROPE Climate, Energy and Mobility grant no. HORIZON-CL5-2023-D1-02-02: C-BLUES, Innovation to advance the evidence base for reporting of BC inventories and greenhouse gas fluxes in coastal wetlands.

**Review statement.** This paper was edited by Tyler Cyronak and reviewed by two anonymous referees.

## References

- Ascough, P., Bompard, N., Garnett, M. H., Gulliver, P., Murray, C., Newton, J.-A., and Taylor, C.:  $^{14}\text{C}$  measurement of samples for environmental science applications at the National Environmental Isotope Facility (NEIF) Radiocarbon Laboratory, SUERC, UK, Radiocarbon, 66, 1020–1031, <https://doi.org/10.1017/RDC.2024.9>, 2024.
- Bao, R., McNichol, A. P., Hemingway, J. D., Gaylord, M. C. L., and Eglinton, T. I.: Influence of Different Acid Treatments on the Radiocarbon Content Spectrum of Sedimentary Organic Matter Determined by RPO/Accelerator Mass Spectrometry, Radiocarbon, 61, 395–413, <https://doi.org/10.1017/RDC.2018.125>, 2019a.
- Bao, R., Zhao, M., McNichol, A., Wu, Y., Guo, X., Haghipour, N., and Eglinton, T. I.: On the Origin of Aged Sedimentary Organic Matter Along a River-Shelf-Deep Ocean Transect, J. Geophys. Res.-Biogeo., 124, 2582–2594, <https://doi.org/10.1029/2019JG005107>, 2019b.
- Bianchi, T. S., Mayer, L. M., Amaral, J. H. F., Arndt, S., Galy, V., Kemp, D. B., Kuehl, S. A., Murray, N. J., and Regnier, P.: Anthropogenic impacts on mud and organic carbon cycling, Nat. Geosci., 17, 287–297, <https://doi.org/10.1038/s41561-024-01405-5>, 2024.
- Boström, B., Comstedt, D., and Ekblad, A.: Isotope fractionation and  $^{13}\text{C}$  enrichment in soil profiles during the decomposition of soil organic matter, Oecologia, 153, 89–98, <https://doi.org/10.1007/s00442-007-0700-8>, 2007.
- Brand, W. A., Coplen, T. B., Vogl, J., Rosner, M., and Prohaska, T.: Assessment of international reference materials for isotope ratio analysis (IUPAC Technical Report), Pure Appl. Chem., 86, 425–467, <https://doi.org/10.1515/pac-2013-1023>, 2014.
- Bromberg, K. D. and Bertness, M. D.: Reconstructing New England salt marsh losses using historical maps, Estuaries, 28, 823–832, <https://doi.org/10.1007/BF02696012>, 2005.
- Campbell, A. D., Fatoyinbo, L., Goldberg, L., and Lagomasino, D.: Global hotspots of salt marsh change and carbon emissions, Nature, 1–6, <https://doi.org/10.1038/s41586-022-05355-z>, 2022.
- Chapman, S. K., Hayes, M. A., Kelly, B., and Langley, J. A.: Exploring the oxygen sensitivity of wetland soil carbon mineralization, Biol. Lett., 15, 20180407, <https://doi.org/10.1098/rsbl.2018.0407>, 2019.
- Dean, J. F., Billett, M. F., Turner, T. E., Garnett, M. H., Andersen, R., McKenzie, R. M., Dinsmore, K. J., Baird, A. J., Chapman, P. J., and Holden, J.: Peatland pools are tightly coupled to the contemporary carbon cycle, Global Change Biology, 30, e16999, <https://doi.org/10.1111/gcb.16999>, 2023.
- Etcheverría, P., Huygens, D., Godoy, R., Borie, F., and Boeckx, P.: Arbuscular mycorrhizal fungi contribute to  $^{13}\text{C}$  and  $^{15}\text{N}$  enrichment of soil organic matter in forest soils, Soil Biol. Biochem., 41, 858–861, <https://doi.org/10.1016/j.soilbio.2009.01.018>, 2009.
- Garnett, M. H., Pereira, R., Taylor, C., Murray, C., and Ascough, P. L.: A New Ramped Oxidation- $^{14}\text{C}$  Analysis Facility at the NEIF Radiocarbon Laboratory, East Kilbride, UK, Radiocarbon, 65, 1213–1229, <https://doi.org/10.1017/RDC.2023.96>, 2023.
- Geraldi, N. R., Ortega, A., Serrano, O., Macreadie, P. I., Lovelock, C. E., Krause-Jensen, D., Kennedy, H., Lavery, P. S., Pace, M. L., Kaal, J., and Duarte, C. M.: Fingerprinting Blue Carbon: Rationale and Tools to Determine the Source of Organic Carbon in Marine Depositional Environments, Front. Marine Sci., 6, 263, <https://doi.org/10.3389/fmars.2019.00263>, 2019.
- Goldstein, A., Turner, W. R., Spawn, S. A., Anderson-Teixeira, K. J., Cook-Patton, S., Fargione, J., Gibbs, H. K., Griscom, B., Hewson, J. H., Howard, J. F., Ledezma, J. C., Page, S., Koh, L. P., Rockström, J., Sanderman, J., and Hole, D. G.: Protecting irrecoverable carbon in Earth's ecosystems, Nat. Clim. Chang., 10, 287–295, <https://doi.org/10.1038/s41558-020-0738-8>, 2020.
- Granse, D., Wanner, A., Stock, M., Jensen, K., and Mueller, P.: Plant-sediment interactions decouple inorganic from organic carbon stock development in salt marsh soils, Limnol. Oceanogr. Lett., 9, 469–477, <https://doi.org/10.1002/lol2.10382>, 2024.
- Griscom, B. W., Adams, J., Ellis, P. W., Houghton, R. A., Lomax, G., Miteva, D. A., Schlesinger, W. H., Shoch, D., Siikamäki, J. V., Smith, P., Woodbury, P., Zganjar, C., Blackman, A., Campari, J., Conant, R. T., Delgado, C., Elias, P., Gopalakrishna, T., Hamisk, M. R., Herrero, M., Kiesecker, J., Landis, E., Laestadius, L., Leavitt, S. M., Minnemeyer, S., Polasky, S., Potapov, P., Putz, F. E., Sanderman, J., Silvius, M., Wollenberg, E., and Fargione, J.: Natural climate solutions, P. Natl. Acad. Sci. USA, 114, 11645–11650, <https://doi.org/10.1073/pnas.1710465114>, 2017.
- Hajdas, I., Ascough, P., Garnett, M. H., Fallon, S. J., Pearson, C. L., Quarta, G., Spalding, K. L., Yamaguchi, H., and Yoneda, M.: Radiocarbon dating, Nat. Rev. Methods Primers, 1, 1–26, <https://doi.org/10.1038/s43586-021-00058-7>, 2021.
- Hansom, J. D. and McGlashan, D. J.: Scotland's coast: Understanding past and present processes for sustainable management, Scottish Geographical Journal, 120, 99–116, 2004.
- Hemingway, J. D.: rampedpyrox: Open-source tools for thermoanalytical data analysis, <http://pypi.python.org/pypi/rampedpyrox> (last access: 10 May 2025), 2016.
- Hemingway, J. D., Galy, V. V., Gagnon, A. R., Grant, K. E., Rosengard, S. Z., Soulet, G., Zigah, P. K., and McNichol, A. P.: Assessing the Blank Carbon Contribution, Isotope Mass Balance, and Kinetic Isotope Fractionation of the Ramped Pyrolysis/Oxidation Instrument at NOSAMS, Radiocarbon, 59, 179–193, <https://doi.org/10.1017/RDC.2017.3>, 2017a.
- Hemingway, J. D., Rothman, D. H., Rosengard, S. Z., and Galy, V. V.: Technical note: An inverse method to relate organic carbon reactivity to isotope composition from serial oxidation, Biogeosciences, 14, 5099–5114, <https://doi.org/10.5194/bg-14-5099-2017>, 2017b.
- Hemingway, J. D., Rothman, D. H., Grant, K. E., Rosengard, S. Z., Eglinton, T. I., Derry, L. A., and Galy, V. V.: Mineral protection regulates long-term global preservation of natural organic carbon, Nature, 570, 228–231, <https://doi.org/10.1038/s41586-019-1280-6>, 2019.

- Houston, A., Garnett, M. H., and Austin, W. E. N.: Blue carbon additionality: New insights from the radiocarbon content of salt-marsh soils and their respired CO<sub>2</sub>, *Limnol. Oceanogr.*, 69, 548–561, <https://doi.org/10.1002/lno.12508>, 2024a.
- Houston, A., Kennedy, H., and Austin, W. E. N.: Additionality in Blue Carbon Ecosystems: Recommendations for a Universally Applicable Accounting Methodology, *Global Change Biol.*, 30, e17559, <https://doi.org/10.1111/gcb.17559>, 2024b.
- Howard, J., Sutton-Grier, A. E., Smart, L. S., Lopes, C. C., Hamilton, J., Kleypas, J., Simpson, S., McGowan, J., Pessarrodona, A., Alleway, H. K., and Landis, E.: Blue carbon pathways for climate mitigation: Known, emerging and unlikely, *Marine Policy*, 156, 105788, <https://doi.org/10.1016/j.marpol.2023.105788>, 2023.
- Komada, T., Bravo, A., Brinkmann, M.-T., Lu, K., Wong, L., and Shields, G.: “Slow” and “fast” in blue carbon: Differential turnover of allochthonous and autochthonous organic matter in minerogenic salt marsh sediments, *Limnol. Oceanogr.*, 67, S133–S147, <https://doi.org/10.1002/lno.12090>, 2022.
- Kwan, V., Friess, D. A., Sarira, T. V., and Zeng, Y.: Permanence risks limit blue carbon financing strategies to safeguard Southeast Asian mangroves, *Commun. Earth Environ.*, 6, 1–8, <https://doi.org/10.1038/s43247-025-02035-4>, 2025.
- Leng, M. J. and Lewis, J. P.: C/N ratios and Carbon Isotope Composition of Organic Matter in Estuarine Environments, in: *Applications of Paleoenvironmental Techniques in Estuarine Studies*, edited by: Weckström, K., Saunders, K. M., Gell, P. A., and Skilbeck, C. G., Springer Netherlands, Dordrecht, 213–237, [https://doi.org/10.1007/978-94-024-0990-1\\_9](https://doi.org/10.1007/978-94-024-0990-1_9), 2017.
- Lilly, A., Baggaley, N., and Donnelly, D.: Map of soil organic carbon in top soils of Scotland, [https://map.environment.gov.scot/Soil\\_maps/?layer=7#](https://map.environment.gov.scot/Soil_maps/?layer=7#) (last access: 17 April 2025), 2012.
- Luk, S. Y., Todd-Brown, K., Eagle, M., McNichol, A. P., Sanderman, J., Gosselin, K., and Spivak, A. C.: Soil Organic Carbon Development and Turnover in Natural and Disturbed Salt Marsh Environments, *Geophys. Res. Lett.*, 48, e2020GL090287, <https://doi.org/10.1029/2020GL090287>, 2021.
- Macreadie, P. I., Anton, A., Raven, J. A., Beaumont, N., Connolly, R. M., Friess, D. A., Kelleway, J. J., Kennedy, H., Kuwae, T., Lavery, P. S., Lovelock, C. E., Smale, D. A., Apostolaki, E. T., Atwood, T. B., Baldock, J., Bianchi, T. S., Chmura, G. L., Eyre, B. D., Fourqurean, J. W., Hall-Spencer, J. M., Huxham, M., Hendriks, I. E., Krause-Jensen, D., Laffoley, D., Luisetti, T., Marbà, N., Masque, P., McGlathery, K. J., Megonigal, J. P., Murdiyarso, D., Russell, B. D., Santos, R., Serrano, O., Silliman, B. R., Watanabe, K., and Duarte, C. M.: The future of Blue Carbon science, *Nat. Commun.*, 10, 3998, <https://doi.org/10.1038/s41467-019-11693-w>, 2019.
- Macreadie, P. I., Costa, M. D. P., Atwood, T. B., Friess, D. A., Kelleway, J. J., Kennedy, H., Lovelock, C. E., Serrano, O., and Duarte, C. M.: Blue carbon as a natural climate solution, *Nat. Rev. Earth Environ.*, 2, 826–839, <https://doi.org/10.1038/s43017-021-00224-1>, 2021.
- Middelburg, J. J., Nieuwenhuize, J., Lubberts, R. K., and van de Plassche, O.: Organic Carbon Isotope Systematics of Coastal Marshes, *Estuar. Coast. Shelf Sci.*, 45, 681–687, <https://doi.org/10.1006/ecss.1997.0247>, 1997.
- Miller, L. C., Smeaton, C., Yang, H., and Austin, W. E. N.: Carbon accumulation and storage across contrasting salt-marshes of Scotland, *Estuar. Coast. Shelf Sci.*, 282, 108223, <https://doi.org/10.1016/j.ecss.2023.108223>, 2023.
- Morris, J. T., Edwards, J., Crooks, S., and Reyes, E.: Assessment of carbon sequestration potential in coastal wetlands, in: *Re-carbonization of the Biosphere: Ecosystems and the Global Carbon Cycle*, edited by: Lal, R., Lorenz, K., Hüttl, R. F., Schneider, B. U., and Braun, J. V., Springer Netherlands, Dordrecht, 517–532, [https://doi.org/10.1007/978-94-007-4159-1\\_24](https://doi.org/10.1007/978-94-007-4159-1_24), 2012.
- Noyce, G. L., Smith, A. J., Kirwan, M. L., Rich, R. L., and Megonigal, J. P.: Oxygen priming induced by elevated CO<sub>2</sub> reduces carbon accumulation and methane emissions in coastal wetlands, *Nat. Geosci.*, 16, 63–68, <https://doi.org/10.1038/s41561-022-01070-6>, 2023.
- Peltre, C., Fernández, J. M., Craine, J. M., and Plante, A. F.: Relationships between Biological and Thermal Indices of Soil Organic Matter Stability Differ with Soil Organic Carbon Level, *Soil Sci. Soc. Am. J.*, 77, 2020–2028, <https://doi.org/10.2136/sssaj2013.02.0081>, 2013.
- Plante, A. F., Fernández, J. M., Haddix, M. L., Steinweg, J. M., and Conant, R. T.: Biological, chemical and thermal indices of soil organic matter stability in four grassland soils, *Soil Biol. Biochem.*, 43, 1051–1058, <https://doi.org/10.1016/j.soilbio.2011.01.024>, 2011.
- Plante, A. F., Beaudré, S. R., Roberts, M. L., and Baisden, T.: Distribution of Radiocarbon Ages in Soil Organic Matter by Thermal Fractionation, *Radiocarbon*, 55, 1077–1083, <https://doi.org/10.1017/S0033822200058215>, 2013.
- Ramnarine, R., Wagner-Riddle, C., Dunfield, K. E., and Voroney, R. P.: Contributions of carbonates to soil CO<sub>2</sub> emissions, *Can. J. Soil. Sci.*, 92, 599–607, <https://doi.org/10.4141/cjss2011-025>, 2012.
- R Core Team: R: A language and environment for statistical computing, R version 4.2.2 (2022-10-31 ucrt), Foundation for Statistical Computing, Vienna, Austria, <https://www.R-project.org/> (last access: 17 April 2025), 2022.
- Reed, D. J., Spencer, T., Murray, A. L., French, J. R., and Leonard, L.: Marsh surface sediment deposition and the role of tidal creeks: Implications for created and managed coastal marshes, *J. Coast. Conserv.*, 5, 81–90, <https://doi.org/10.1007/BF02802742>, 1999.
- Rosengard, S. Z., Mauro S. Moura, J., Spencer, R. G. M., Johnson, C., McNichol, A., Boehman, B., and Galy, V.: The Thermal Reactivity and Molecular Diversity of Particulate Organic Carbon in the Amazon River Mainstem, *J. Geophys. Res.-Biogeo.*, 130, e2024JG008660, <https://doi.org/10.1029/2024JG008660>, 2025.
- Rosenheim, B. E., Day, M. B., Domack, E., Schrum, H., Benthien, A., and Hayes, J. M.: Antarctic sediment chronology by programmed-temperature pyrolysis: Methodology and data treatment, *Geochem. Geophys. Geosyst.*, 9, <https://doi.org/10.1029/2007GC001816>, 2008.
- Saintilan, N., Rogers, K., Mazumder, D., and Woodroffe, C.: Allochthonous and autochthonous contributions to carbon accumulation and carbon store in southeastern Australian coastal wetlands, *Estuar. Coast. Shelf Sci.*, 128, 84–92, <https://doi.org/10.1016/j.ecss.2013.05.010>, 2013.
- Sanderman, J. and Grandy, A. S.: Ramped thermal analysis for isolating biologically meaningful soil organic matter

- fractions with distinct residence times, *SOIL*, 6, 131–144, <https://doi.org/10.5194/soil-6-131-2020>, 2020.
- Sasmito, S. D., Taillardat, P., Adinugroho, W. C., Krisnawati, H., Novita, N., Fatoyinbo, L., Friess, D. A., Page, S. E., Lovelock, C. E., Murdiyarso, D., Taylor, D., and Lupascu, M.: Half of land use carbon emissions in Southeast Asia can be mitigated through peat swamp forest and mangrove conservation and restoration, *Nat. Commun.*, 16, 740, <https://doi.org/10.1038/s41467-025-55892-0>, 2025.
- Schmidt, M. W. I., Torn, M. S., Abiven, S., Dittmar, T., Guggenberger, G., Janssens, I. A., Kleber, M., Kögel-Knabner, I., Lehmann, J., Manning, D. A. C., Nannipieri, P., Rasse, D. P., Weiner, S., and Trumbore, S. E.: Persistence of soil organic matter as an ecosystem property, *Nature*, 478, 49–56, <https://doi.org/10.1038/nature10386>, 2011.
- Smeaton, C., Garrett, E., Koot, M. B., Ladd, C. J. T., Miller, L. C., McMahon, L., Foster, B., Barlow, N. L. M., Blake, W., Gehrels, W. R., Skov, M. W., and Austin, W. E. N.: Organic carbon accumulation in British saltmarshes, *Sci. Total Environ.*, 926, 172104, <https://doi.org/10.1016/j.scitotenv.2024.172104>, 2024.
- Soldatova, E., Krasilnikov, S., and Kuzyakov, Y.: Soil organic matter turnover: Global implications from  $\delta^{13}\text{C}$  and  $\delta^{15}\text{N}$  signatures, *Sci. Total Environ.*, 912, 169423, <https://doi.org/10.1016/j.scitotenv.2023.169423>, 2024.
- Spivak, A. C., Sanderman, J., Bowen, J. L., Canuel, E. A., and Hopkinson, C. S.: Global-change controls on soil-carbon accumulation and loss in coastal vegetated ecosystems, *Nat. Geosci.*, 12, 685–692, <https://doi.org/10.1038/s41561-019-0435-2>, 2019.
- Spohn, M., Babka, B., and Giani, L.: Changes in soil organic matter quality during sea-influenced marsh soil development at the North Sea coast, *CATENA*, 107, 110–117, <https://doi.org/10.1016/j.catena.2013.02.006>, 2013.
- Stoner, S. W., Schrumpf, M., Hoyt, A., Sierra, C. A., Doetterl, S., Galy, V., and Trumbore, S.: How well does ramped thermal oxidation quantify the age distribution of soil carbon? Assessing thermal stability of physically and chemically fractionated soil organic matter, *Biogeosciences*, 20, 3151–3163, <https://doi.org/10.5194/bg-20-3151-2023>, 2023.
- Systat Software Inc: Sigmaplot v12.5, <https://grafiti.com/> (last access: 17 April 2025), 2013.
- Van Dam, B. R., Zeller, M. A., Lopes, C., Smyth, A. R., Böttcher, M. E., Osburn, C. L., Zimmerman, T., Pröfrock, D., Fourqurean, J. W., and Thomas, H.: Calcification-driven  $\text{CO}_2$  emissions exceed “Blue Carbon” sequestration in a carbonate seagrass meadow, *Sci. Adv.*, 7, eabj1372, <https://doi.org/10.1126/sciadv.abj1372>, 2021.
- Van de Broek, M., Vandendriessche, C., Poppelmonde, D., Merckx, R., Temmerman, S., and Govers, G.: Long-term organic carbon sequestration in tidal marsh sediments is dominated by old-aged allochthonous inputs in a macrotidal estuary, *Global Change Biol.*, 24, 2498–2512, <https://doi.org/10.1111/gcb.14089>, 2018.
- VERRA: VM0033 Methodology for Tidal Wetland and Seagrass Restoration, v2.1, <https://verra.org/methodologies/vm0033-methodology-for-tidal-wetland-and-seagrass-restoration-v2-1/> (last access: 17 April 2025), 2023.
- Werth, M. and Kuzyakov, Y.:  $^{13}\text{C}$  fractionation at the root–microorganisms–soil interface: A review and outlook for partitioning studies, *Soil Biol. Biochem.*, 42, 1372–1384, <https://doi.org/10.1016/j.soilbio.2010.04.009>, 2010.
- Williams, E. K. and Rosenheim, B. E.: What happens to soil organic carbon as coastal marsh ecosystems change in response to increasing salinity? An exploration using ramped pyrolysis, *Geochem. Geophys. Geosyst.*, 16, 2322–2335, <https://doi.org/10.1002/2015GC005839>, 2015.